Identification of the differentially expressed genes in the leg muscles of Zhedong white geese (*Anser cygnoides*) reared under different photoperiods

Moran Hu [1], Hangfeng Jin,[1] Jianqing Wu, Xiaolong Zhou, Songbai Yang, Ayong Zhao, and Han Wang [2]

Key Laboratory of Applied Technology on Green-Eco Healthy Animal Husbandry of Zhejiang Province, College of Animal Science and Technology, College of Veterinary Medicine, Zhejiang A&F University, Zhejiang 311300, China

ABSTRACT Light is a factor affecting muscle development and meat quality in poultry production. However, few studies have reported on the role of light in muscle development and meat quality in geese. In this experiment, 10 healthy 220-day-old Zhedong white geese were reared for 60 d under a long photoperiod (15L:9D, **LL**) and short photoperiod (9L:15D, **SL**). The gastrocnemius muscles were collected after slaughter to evaluate muscle fiber characteristics and meat color, and RNA-seq analysis. The results showed that compared to the LL group, the SL group had large muscle fiber diameter and cross-sectional area, few muscle fibers per unit area, high meat color a* value, and low L* value at 24 h postmortem. On comparing the 2 groups, 70 differentially expressed genes (**DEGs**) were identified. Compared to the SL group, the LL group had 25 upregulated and 45 downregulated genes. Gene Ontology (**GO**) enrichment analysis showed that these DEGs were mainly involved in cell, cell part, binding, cellular processes, and single-organism processes. Several significantly enriched athways were identified in the Kyoto Encyclopedia of Genes and Genomes (**KEGG**) pathway analysis, such as the calcium and PI3k-Akt signaling pathways. The expression of five randomly selected DEGs was verified using quantitative real-time PCR, and the results were consistent with the RNA-seq data. This study provides a theoretical basis for studying the molecular mechanisms by which light affects muscle development and meat color in geese.

Key words: muscle development, meat color, Zhedong White Geese, photoperiod, RNA-seq

2022 Poultry Science 101:102193
https://doi.org/10.1016/j.psj.2022.102193

INTRODUCTION

In the global meat market, goose meat is an excellent source of high-quality protein which contains all kinds of amino acids needed by humans (Haraf et al., 2021). The ideal high protein, low fat, and low cholesterol levels makes goose meat a popular nutritional health food among consumers (Buzała et al., 2014; Journal, 2021; Orkusz, 2021). China is the largest producer and consumer of goose meat globally. However, owing to the lack of a scientific breeding method, the breeding cycle of geese is longer than that of other poultry, which seriously restricts the development of the goose industry (Gao et al., 2021a). Therefore, exploring scientific methods to improve muscle development and meat quality of Chinese local geese is a useful way to overcome the current predicament.

Changes in photoperiod affect animal behavior, growth, food intake, and reproductive status (Mariné-Casadó et al., 2018). Atlantic salmon treated with continuous light showed an increased rate of muscle fiber recruitment, a high proportion of fast-twitch fibers, and a rapid increase in the muscle fiber cross-sectional area (Johnston et al., 2003). In addition, photoperiod induced weight gain and insulin-like growth factor-I (**IGF-I**) levels in the muscle of mice (Chennaoui et al., 2017). Monochromatic green light stimulation promotes the expression of the growth hormone/insulin-like growth factor-I (GH-IGF-I) axis and activates muscle satellite cell proliferation and myofibril formation in chick embryos (Bai et al., 2019). However, there are few reports on whether photoperiod affects muscle development in geese. Exploring a reasonable and effective light regime may be an important research direction for improving the production performance of geese.

Meat color is one of the key indicators for consumers to evaluate the quality of meat and also is one of the most important quality traits influencing consumer purchasing decisions (You et al., 2020). In poultry production, light is a key factor affecting the poultry meat color. Long light exposure reduces the redness of broiler meat (Tuell et al., 2020a). It is better to use intermittent

Received May 10, 2022.
Accepted September 16, 2022.

[1]These contributed equally to this work.

[2]Corresponding author: wanghan1990@zafu.edu.cn

light during duck feeding or only short light in the early stages to maintain a higher redness value of duck meat (Starčević et al., 2021). Dim light reduces the brightness of broiler meat color (Fidan et al., 2017), whereas long light makes the chicken meat color lighter and increases muscle lipid oxidation and protein denaturation (Tuell et al., 2020b). Prolongation of the photoperiod may negatively affect muscle oxidative stability and color by altering muscle metabolites (Tuell et al., 2020a). However, whether light affects geese meat color and the underlying molecular mechanisms by which light rgulates poultry meat color remain to be further investigated.

Since RNA-seq technology was proposed in 2008, it has been widely used in biological research, medical diagnosis and treatment (Ghosh et al., 2018; Kloet et al., 2020). RNA-seq technology has been used to compare the skeletal muscle transcriptomes of Muscovy ducks at different developmental stages and many potential candidate genes have been identified (Hu et al., 2020). In a study of chicken meat color, 1,317 candidate genes related to glycolysis, fatty acid metabolism, and protein metabolism, were screened using RNA-seq technology (Sun et al., 2022). In addition, 397 differentially methylated genes highly correlated with cellular metabolic processes were identified after m6A transcriptome sequencing of the pectoralis muscle in Ding'an geese (Xu et al., 2021). Thus, whole genome sequencing technology plays an important role in exploring the molecular mechanism of poultry traits.

In this study, the Chinese local breed Zhedong White Geese was used as the experimental object. High-throughput sequencing technology and bioinformatics were used to identify differentially expressed genes and signaling pathways present in the gastrocnemius muscles of geese reared under different photoperiod conditions. The results of this study provide a theoretical basis for improving the meat production performance of geese.

MATERIALS AND METHODS

Experimental Animals and Tissues

The Zhedong white geese (*Anser cygnoides*) used in this study were raised at the East Zhejiang White Geese Original Breeding Farm, Xiangshan County, Zhejiang Province, China. Twenty healthy 220-day-old Zhedong white goose females with similar weights were randomly divided into 2 groups. One group was kept under a long photoperiod (15L:9D, LL) and the other was kept under a short photoperiod under (9L:15D, SL) using artificial light controlled at 30 lx. After 60 d of feeding, 6 geese were dissected from each group and leg muscle samples were collected. All samples were immediately frozen in liquid nitrogen and stored at −80°C until use.

All animal experimental procedures used in this study were approved by the Ethics Committee for Animal Experiments of Zhejiang A&F University and were performed in accordance with the Guidelines for Animal Experimentation of the University (Hangzhou, China).

Total RNA Extraction, Library Construction, and Sequencing

Total RNA was extracted from the gastrocnemius muscle of the legs using the TRIzol method (Puch-Hau et al., 2019). To ensure that the samples qualified, quality testing was performed by the sample testing center of Majorbio Bio-pharm Technology Co., Ltd. (Shanghai, China). The quality reports are presented in Table S1. All RNA samples met the requirements for Optical density (**OD**) values (260/280 > 2.0) for further analysis. The RNA-seq transcriptome library was prepared using the TruSeq RNA sample preparation Kit from Illumina (San Diego, CA) using 1 μg of total RNA. Briefly, messenger RNA was isolated according to the polyA selection method using oligo (dT) beads and then fragmented using fragmentation buffer. Second, double-stranded cDNA was synthesized using a SuperScript double-stranded cDNA synthesis kit (Invitrogen, CA) with random hexamer primers (Illumina). The synthesized cDNA was then subjected to end-repair, phosphorylation, and 'A' base addition according to Illumina's library construction protocol. Libraries were selected for cDNA target fragments of 300 bp on 2% low range ultra-agarose, followed by PCR amplification using Phusion DNA polymerase (NEB) for 15 PCR cycles. After quantification using TBS380, the paired-end RNA-seq sequencing library was sequenced using the Illumina HiSeq xten/NovaSeq 6000 sequencer (2 × 150 bp read length). Goose leg muscles of the SL group were numbered sl 1, sl 2, and sl 3, and those of the LL group were numbered ll 1, ll 2, and ll 3, for subsequent analysis.

Sequencing Quality Assessment and Differentially Expressed Gene

Screening The SeqPrep and Sickle software were used to remove low quality reads from the raw data. Q20, Q30, GC content, and sequence repeat levels were calculated using fastp. All downstream analyses were based on high-quality clean reads. The goose genome sequences were downloaded from the NCBI database (https://www.ncbi.nlm.nih.gov/genome/31397?genome_assembly_id=229313). The resulting clean reads were compared with the reference genome of the goose using Hisat2.

To identify differentially expressed genes (**DEGs**) between the 2 groups, the expression level of each transcript was calculated according to the transcripts per million reads (**TPM**) method. RSEM (http://deweylab.biostat.wisc.edu/rsem/) (Dewey and Li, 2011) was used to quantify gene abundances. Differential expression analysis was performed using the DESeq2 (Love et al., 2014), DEGseq (Wang et al., 2010), and EdgeR (Robinson et al., 2010) method. Differentially expressed genes with |log2FC|>1 and Q value ≤ 0.05

(DESeq2 or EdgeR) or Q value ≤ 0.001 (DEGseq) were considered to be significantly differentially expressed.

Gene Ontology and Kyoto Encyclopedia of Genes and Genomes Pathway Enrichment Analysis

The Goatools based on the Gene Ontology (**GO**) database (http://www.geneontology.org/) were used to analyze the GO enrichment. Three parts, Biological Process (**BP**), Molecular Function (**MF**), and Cellular Component (**CC**) were used for classification annotation. Based on the Kyoto Encyclopedia of Genes and Genomes (**KEGG**) database (http://www.genome.jp/kegg/), we used the KOBAS software (2.1, Peking University, China) to test the statistical enrichment of DEGs in the KEGG pathways.

Quantitative Real-Time PCR

Using the NCBI gene library, primers of 5 randomly selected DEGs and the house-keeping gene GAPDH were designed using Primer Premier 5 software (Table 1). Primers were synthesized by Hangzhou Youkang Biotechnology Co., Ltd. Total RNA was used to synthesize cDNA using the 5 × All-In-One MasterMix Kit (ABM, Zhengjiang, China). As the template, cDNA was used for quantitative PCR using the EvaGreen 2 × qPCR MasterMix Kit (ABM). Three replicates were performed for each sample. The relative expression of each gene was calculated using $2^{-\triangle\triangle CT}$ statistical analysis. All data are shown as mean ± SEM, and unpaired Student's t tests were used to calculate P-values.

Analysis of Muscle Structure

Goose leg muscle samples were fixed with 4% paraformaldehyde and embedded in paraffin blocks. After the paraffin block was sectioned (5 μm), it was stained with hematoxylin and eosin solution, and the slides were placed in 70% ethanol for 20 s, 90% ethanol for 20 s, 100% ethanol for 1 min, and xylene for 3 min, and then air-dried and sealed (Wang et al., 2017). Sections were photographed using a fluorescence microscope (Olympus, Tokyo, Japan). Three samples were obtained from each group of geese, and 5 micrographs were randomly selected for each sample. A total of 90 muscle fibers per group were counted using the ImageJ software, and the average of 5 measurements was taken as the fiber cross-sectional area (μm^2), diameter (μm), and density (fibers/mm^2) (Zhang et al., 2014).

Table 1. Primers used in the real-time PCR.

Gene name	Sequence (5'-3')	Product size
GAPDH	F: TTCCTCCACCTTTGATGCGG R:ACCATCAAGTCCACCACACG	114bp
PHKB	F:CAACAATGGCAGTCCAGAGC R:TTGGGTACAACAGGACACCC	543bp
SOX6	F:TGGCTGGTGTGGTAGGAG R:AGGCAGATGAGAGGTCGC	188bp
GCK	F:GCAGAAAGTGGAGATGGA R:GTGACACGGGAAAGAGAA	172bp
HSPB1	F:GTATTTCCGTCTGCTGCC R:TGTTTCTCCTCGTGCTTG	222bp
PHGDH	F:TGAAGGAAGGCAAATGGG R:GGTCTCGGGGGTGATGAT	164bp

RESULTS

Differences in Muscle Fiber Characteristics of Goose Leg Muscles Under Different Photoperiods

To explore the effect of photoperiod on muscle fiber characteristics in geese, gastrocnemius muscles were sectioned and stained. The results showed that the density of muscle fibers in the SL group was lower than that in the LL group, but the cross-sectional area and diameter of the muscle fibers were larger (Figures 1A−1D). Therefore, it was inferred that SL may promote goose muscle hypertrophy.

Effect of Different Photoperiods on Meat Color of Geese

To investigate whether light affects geese meat color, meat color measurements were performed of leg muscles of geese reared under different photoperiods (Figure 2). The results showed that SL significantly reduced the L* value (brightness) (P-value = 0.025) while increasing the a* value (redness) (P-value = 0.0315) of goose meat color compared to that under LL (Table 2).

Sequencing Quality Evaluation

During the sequencing process, the raw data were quality controlled and a quality assessment was provided to ensure the accuracy of the subsequent analysis. The results listed in Table 3 show that the values of Q20 (base quality > 20 and error rate < 0.01)) are all above 98% and those of Q30 (base quality > 30 and error rate < 0.001) are all above 94%. The GC content ranged from 53 to 57%. The results indicated that the data had a low probability of error which met the sequencing requirements.

More than 68% of the reads were aligned to the reference genome and 65 to 75% of the clean reads

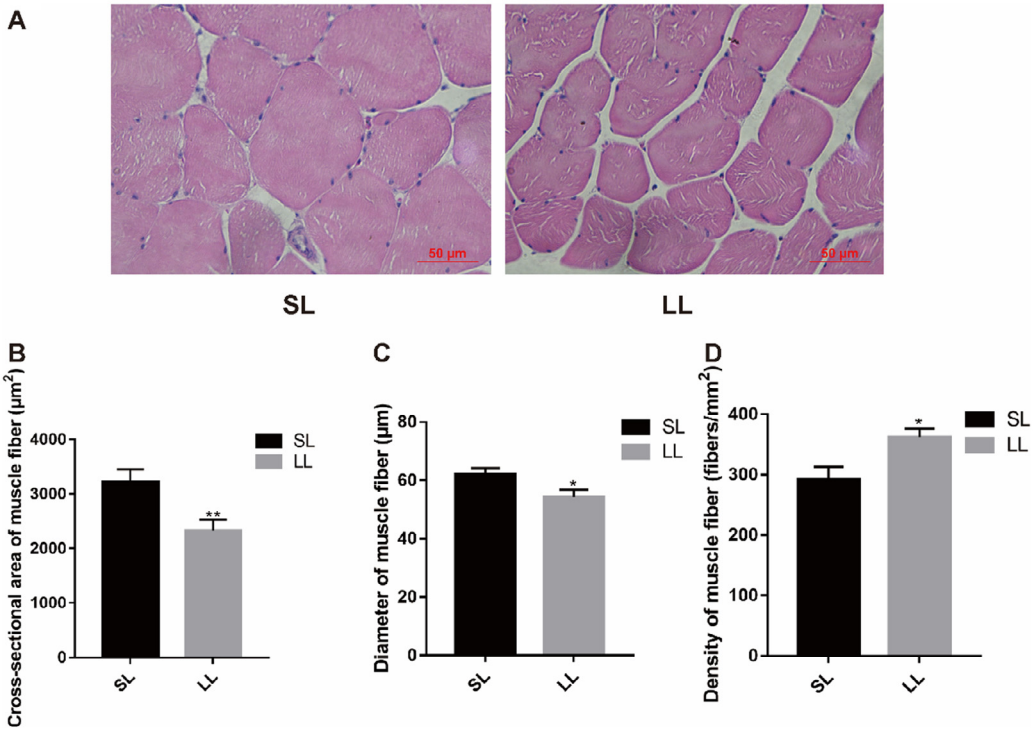

Figure 1. Muscle fiber characteristics of geese under different photoperiods. (A) Representative micrographs of hematoxylin and eosin (H&E) staining of leg muscles of geese reared under different photoperiods. (B) Measurement of cross-sectional area of leg muscle fibers of geese reared under different photoperiods. (C) Measurement of the diameter of leg muscle fibers of geese reared under different photoperiods. (D) Measurement of the number of muscle fibers per unit area of leg muscles of geese reared under different photoperiods. ** $P < 0.01$, * $P < 0.05$, n = 6.

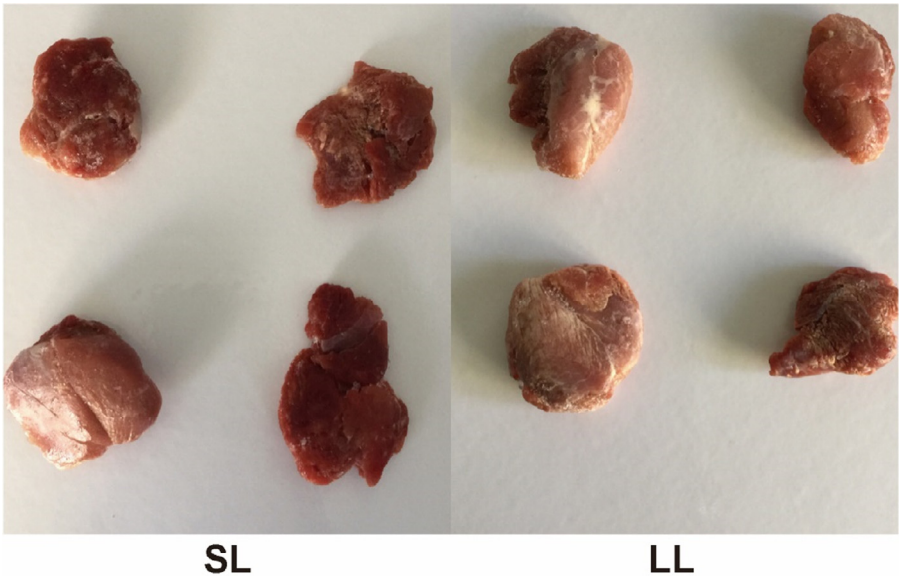

Figure 2. Gastrocnemius muscle of Zhedong White geese in the two groups. n = 4.

Table 2. L* (brightness), a* (redness) and b* (yellowness) values of goose leg muscles at 24 h postmortem under different photoperiods (n = 10).

Light/h	Brightness L*	Redness a*	Yellowness b*
15h	26.65 ± 1.21[a]	55.91 ± 0.81[b]	15.26 ± 0.59
9h	23.49 ± 1.60[b]	58.30 ± 1.40[a]	15.23 ± 1.19
P-value	0.0250	0.0315	0.4830

[a-b]In the same column, values with different lowercase superscripts indicate significant differences (P < 0.05).

had unique comparison positions on the reference genome (Table 4). This illustrates that the clean reads obtained were available for post-sequencing analysis.

Correlation analysis was performed to assess the quality of repeatability within the group. The results showed that there were differences between the groups and the biological replicates within the groups were good (Figure 3).

Table 3. Quality assessment of sequencing date.

Sample	Clean reads	Clean bases	Q20(%)	Q30(%)	GC content(%)
sl_1	54,313,760	80,26,863,149	98.27	95.01	54.53
sl_2	44,389,142	6,555,398,259	98.35	95.26	56.73
sl_3	48,539,644	7,211,649,150	98.75	95.98	54.97
ll_1	46,095,306	6,861,678,422	98.76	95.99	54.88
ll_2	51,839,210	7,677,991,815	98.25	94.95	54.92
ll_3	49,484,182	7,363,615,166	98.74	95.92	53.94

sl and ll represent short and long photoperiod groups, respectively. 1/2/3 represent three biological replicates for each group. Clean reads: total number of sequencing data entries after quality control. Clean bases: total sequencing data volume after quality control (i.e., number of clean reads multiplied by the length of reads). Q20 and Q30: the percentage of bases with sequencing quality above 99% and 99.9% of the total bases, respectively. GC content: Quality control (QC) data corresponded to the sum of G and C bases as a percentage of the total bases.

Screening of DEGs

The total number of genes screened by RNA-Seq was 9,858. To display gene expression distribution, a volcano plot was constructed using -log10 (adjusted) as the vertical coordinate and log2 (FC) as the horizontal coordinate (Figure 4A). A total of 70 DEGs were identified. There were 45 upregulated genes and 25 downregulated genes in the SL group compared to the LL group (Figure 4A). The expression levels of 5 randomly selected DEGs, including 3 downregulated genes (GCK, HSPB1, and PHGDH) and 2 upregulated genes (PHKB and SOX6), were verified using quantitative real-time PCR. The results showed that their expression trends

Table 4. Statistical results of the comparison with the reference genome.

Sample	Total reads	Total mapped	Multiple mapped	Uniquely mapped
sl_1	54,313,760	40,223,184(74.06%)	1,160,976(2.14%)	39,062,208(71.92%)
sl_2	44,389,142	30,206,700(68.05%)	1,050,449(2.37%)	29,156,251(65.68%)
sl_3	48,539,644	35,760,428(73.67%)	1,084,433(2.23%)	34,675,995(71.44%)
ll_1	46,095,306	34,149,665(74.08%)	1,158,824(2.51%)	32,990,841(71.57%)
ll_2	51,839,210	37,800,821(72.92%)	14,66,913(2.83%)	36,333,908(70.09%)
ll_3	49,484,182	37,292,580(75.36%)	11,01,398(2.23%)	36,191,182(73.14%)

sl and ll represent short and long photoperiod groups, respectively. 1/2/3 represent three biological replicates for each group. Total reads: total number of sequencing data entries after quality control (i.e., clean reads). Total mapped: number of clean reads localized to the genome. Multiple mapped: number of clean reads with multiple comparison positions in the reference sequence. Uniquely mapped: number of clean reads with a unique comparison position on the reference sequence.

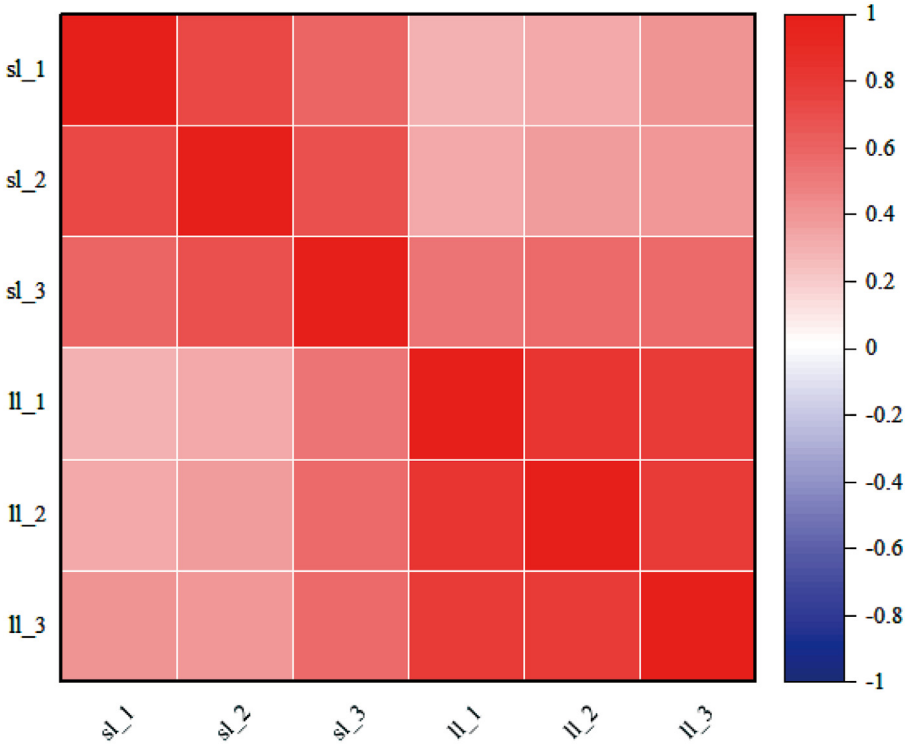

Figure 3. Heat map of intersample correlation.

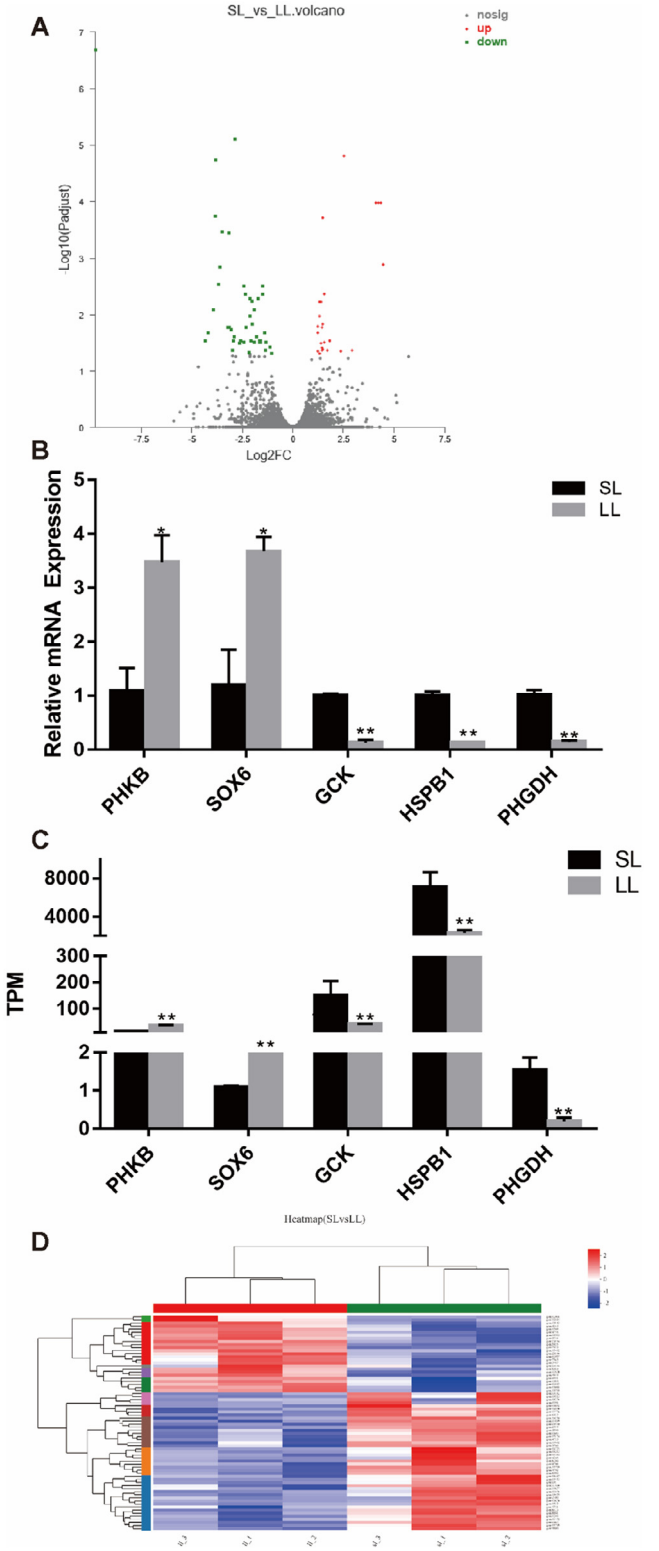

Figure 4. Differential gene expression (DEGs) analysis. (A) Volcano plot for differential gene expression. (B) Validation of DEGs by qRT-PCR. (C) DEGs in RNA-seq results. (D) Heat map of differential gene expression. ** $P < 0.01$, * $P < 0.05$, n = 3.

were highly consistent with the sequencing results, which proved the reliability of the microarray analysis (Figures 4B and 4C).

To ensure the accuracy of the analysis, the screened differentially expressed genes were subjected to hierarchical clustering analysis. The horizontal coordinates represent sample clustering. One column represents one sample, and clustering analysis was based on the similarity of gene expression patterns between samples. The closer the distance, the more similar were the samples (Figure 4D). These results suggests that these DEGs clearly divided the leg muscle samples into short and long photoperiod groups, indicating the reliability of our analysis.

GO Annotation and Enrichment Analysis

To further reveal the molecular characterization of these DEGs, they were analyzed using GO annotations. The results showed that 70 DEGs were annotated with 20 GO terms, including 11 biological processes, 7 cellular components, and 2 molecular function annotations. The major GO terms were significantly enriched in biological processes, which included positive regulation of biological processes, localization, development process, multicellular organismal process, signaling, response to stimulus, metabolism, regulation of biological processes, biological regulation, cellular processes, and single-organism processes. In addition, macromolecular complexes, membrane, extracellular region, extracellular region part, organelles, and cell part and cells were enriched among cellular components. The main functional term of molecular function were catalytic activity and binding, which were enriched in 11 and 24 genes, respectively (Figure 5).

KEGG Pathway Enrichment Analysis

To understand the signaling pathways in which the genes were distributed, a KEGG pathway analysis was performed. A total of 48 DEGs were mapped to 127 KEGG pathways, of which 20 were significantly enriched ($P < 0.05$). There were several significantly enriched signaling pathways, including amoebiasis, the calcium signaling pathway, and the PI3k-Akt signaling pathway (Figure 6).

DISCUSSION

Light plays an important role in goose productions and metabolism. Reasonable and effective use of light can greatly affect the production performance of geese (Wang et al., 2009; Liu et al., 2020). The present study showed that the Zhedong white geese in the SL group had a larger muscle fiber diameter and cross-sectional area, but had a smaller number of muscle fibers per unit area than those in the LL group. Melatonin levels in the blood of geese increase under dark conditions (Zawilska et al., 2003). Melatonin can promote proliferation of skeletal muscle satellite cells (Lamosová et al., 1998). Long-term exogenous addition of melatonin effectively prevents muscle atrophy (Lee et al., 2012). Therefore, melatonin may be a key hormone in light-induced muscle hypertrophy in geese. Our study also found that the meat color of geese under SL had a higher a*

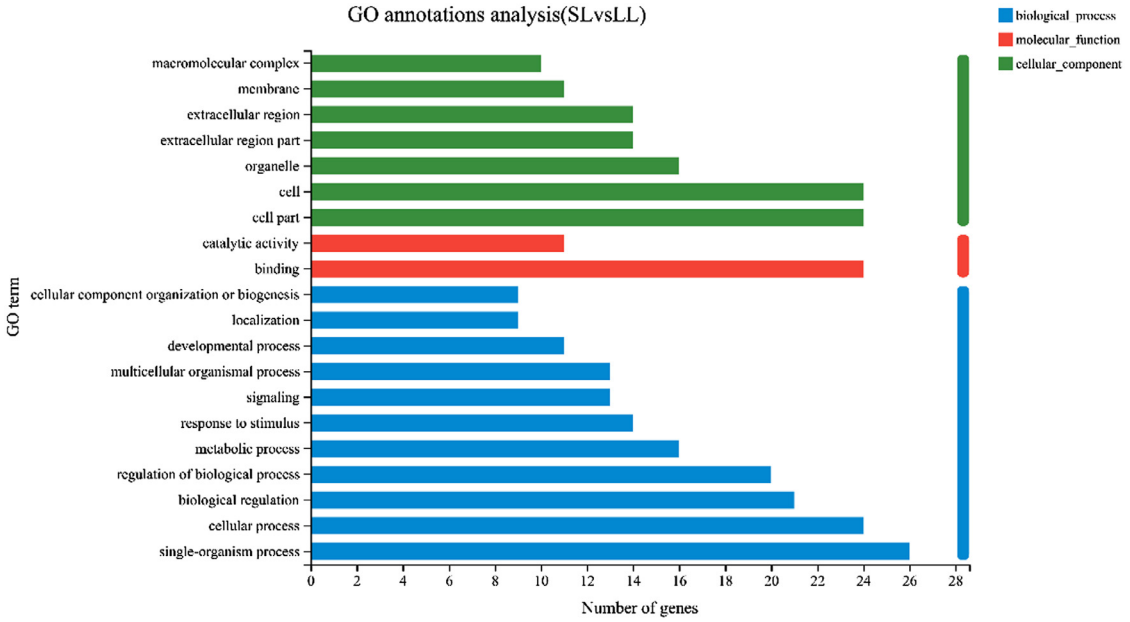

Figure 5. GO annotations analysis of the DEGs. Abbreviation: DEGs, differential gene expression.

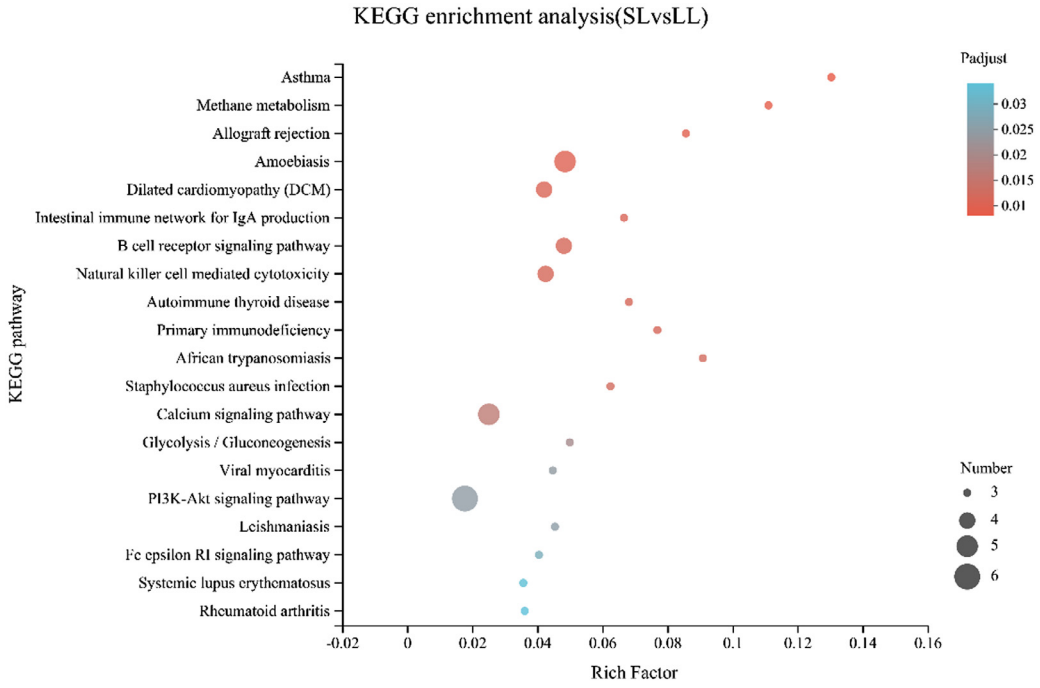

Figure 6. Top 20 significantly enriched KEGG pathways.

parameter and lower L* parameter than those under LL conditions, thus having a high commercial value. Glucocorticoid downregulation in birds is caused by prolonged light exposure (House et al., 2021). In muscle cells, increased glucocorticoid levels reduce cellular respiration and shift the cellular metabolic phenotype to glycolysis (Torres-Velarde et al., 2021). Studies have shown that glycolysis is an important metabolic pathway that affects meat color, and meat with low glycolytic dehydrogenase activity has poor color stability (Xin et al., 2018; Gao et al., 2021b). Through RNA-seq analysis of leg muscles of geese reared under different photoperiods, 70 DEGs were identified, among which 5 DEGs were randomly selected for further verification of expression levels using qRT-PCR. Although the expression levels of the genes selected by the 2 methods were different, their expression trends were highly consistent, which proved the reliability of the sequencing analysis results.

The basic processes of muscle development in geese include cellular and biological processes and biological regulation. GO annotation analysis showed that 20 DEGs were enriched in the GO term: regulation of biological processes (Table S2). Among these DEGs, FMOD, HSPB1, and STC1 were upregulated in the goose leg muscles under SL condtions. FMOD promotes chicken myogenic cell differentiation and alleviates muscle atrophy (Yin et al., 2020). Inhibition of HSPB1 during myogenesis represses myotube formation (Kim et al.,

2018). STC1 can accelerate the fusion of mouse muscle cells to form myotubes (Jiang et al., 2000). In addition, NOV, PHGDH, and TNNT2 were also identified as upregulated DEGs in goose leg muscles under SL conditions. Loss of the NOV gene in mice causes muscle wasting (Heath et al., 2008). Our previous study indicated that PHGDH promoted the proliferation of chicken skeletal muscle satellite cells (Wang et al., 2022). TNNT2 is an important gene that induces grouper myoblasts differentiation (Kong et al., 2021). Polymorphism in the TNNT2 gene was closely associated with the pork color b* parameter (Ropka-Molik et al., 2018), which provided a theoretical basis for our subsequent study on the role of TNNT2 in light-influenced muscle development and meat color chage in geese. In contrast, KCNJ2 was significantly downregulated under SL conditions. Mutations in KCNJ2 cause malformations in muscle development (Andelfinger et al., 2002). Therefore, we speculated that these genes may play a key role in the regulation of goose myoblast differentiation and muscle hypertrophy.

The energy metabolism of muscle after slaughter affects meat color (Men et al., 2017). GO annotation analysis revealed that 16 DEGs were enriched in metabolic process-related GO terms (Table S2). Inhibition of glycolysis in the skeletal muscle has been reported to increase glycogen synthesis (Clark et al., 1987; Ren et al., 1993). Research has shown that animals with high glycogen levels tend to have worse meat color at 24 h postmortem (Choe et al., 2008). ACSL6, AGL, and GPD2 were upregulated in the LL group. Inhibition of ACSL6 reduces glucose uptake in the skeletal muscle (Jung and Bu, 2020), which in turn reduces muscle glycogen synthesis (Ryder et al., 1999). Cancer cells with knockout of AGL expression were more metabolically active and dependent on glycolysis than cells that express AGL normally (Lew et al., 2015). GPD2 can inhibit glycolysis in tumor cells (Wu et al., 2020; Zhao et al., 2021). In our study, the KEGG pathway enrichment analysis results indicated that the 2 most significantly enriched pathways were related to the energy metabolism in muscles (Table S3). ALDOC is active during the second stage of glycolysis (Wang et al., 2007). Knockdown of ALDOC significantly inhibits MUC16C-induced glycolysis in tumors (Fan et al., 2020). Thus, we inferred that these DEGs were activated during the process of light exposure, affecting goose meat color.

After animal death, mitochondria continue to metabolize oxygen in the skeletal muscle (Tang et al., 2005). Mitochondrial oxygen depletion establishes anaerobic conditions that promote the reduction of MetMb by transferring electrons from NADH or succinate to oxygen (Watts et al., 2010), which improves meat color stability. HSPB1 was upregulated in the SL group and was significantly enriched in GO term metabolic processes (Table S2). HSPB1 was found to restore the mitochondrial respiratory impairment caused by cellular stress (Mule et al., 2021). Pyruvate, a product of glycolysis, supports mitochondrial respiration in postmortem muscles (Mohan et al., 2010). GCK was significantly enriched in the glycolysis/gluconeogenesis pathway (Table S3) and highly expressed under SL conditions. During normal hepatocellular carcinogenesis, GCK expression can link the central carbon metabolism and stimulate mitochondrial respiration (Perrin-Cocon et al., 2021). Thus, these DEGs may be involved in the process of light affecting goose meat color through mitochondrial respiration.

KEGG enrichment analysis showed that the DEGs were significantly enriched in the calcium signaling pathway (Table S3). The intracellular calcium signaling pathway is an important factor that influences meat color (Lonergan et al., 2003; Ropka-Molik et al., 2017). Among the genes upregulated in the LL group, PHKB was significantly enriched in the calcium signaling pathway (Table S3). PHKB is a key regulatory enzyme in glycogen metabolism (Wüllrich-Schmoll and Kilimann, 1996), and mutations in PHKB can lead to the accumulation of muscle glycogen (Burwinkel et al., 1997). Muscles with high glycogen levels usually show a poor meat color at 24 h postmortem (Choe et al., 2008). In addition, the present study found that DEGs were significantly enriched in the PI3K-Akt signaling pathway (Table S3). FIGF was upregulated in the LL group. A C>G mutation in the bird FIGF gene results in a dramatic increase in the number of muscle fibers (Chen et al., 2013). The number of muscle fibers per unit area was higher in the LL group, which may be correlated with the function shown in FIGF.

Future research will be directed at determining the optimal photoperiods to utilize these DEGs and signaling pathways to regulate goose muscle development and quality to enable further rapid development of the goose industry.

CONCLUSIONS

The present study demonstrated that short light significantly promoted goose muscle development, resulting in a larger cross-sectional area and diameter of muscle fibers. In addition, short light remarkably improved the redness of goose meat. RNA-seq analysis provided a catalog of mRNAs for the study of the mechanisms by which light affects muscle development and meat color in geese, and screened 3 signaling pathways (glycolysis/gluconeogenesis, calcium signaling pathway, and PI3K-Akt signaling pathway) that may be involved in this regulation. The experimental data provided a theoretical basis for studying the molecular mechanisms by which light affects muscle development and meat color in geese.

ACKNOWLEDGMENTS

This work was supported by the National Natural Science Foundation of China (NO. 31872397).

DISCLOSURES

The authors declare that there is no conflict of interest regarding the publication of this paper.

SUPPLEMENTARY MATERIALS

Supplementary material associated with this article can be found in the online version at doi:10.1016/j.psj.2022.102193.

REFERENCES

Andelfinger, G., A. R. Tapper, R. C. Welch, C. G. Vanoye, A. L. George Jr, and D. W Benson. 2002. KCNJ2 mutation results in Andersen syndrome with sex-specific cardiac and skeletal muscle phenotypes. Am. J. Hum. Genet 71:663–668.

Bai, X., J. Cao, Y. Dong, Z. Wang, and Y. J. P. O. Chen. 2019. Melatonin mediates monochromatic green light-induced satellite cell proliferation and muscle growth in chick embryo. PLoS One 14: e0216392.

Burwinkel, B., A. J. Maichele, O. Aagenaes, H. D. Bakker, A. Lerner, Y. S. Shin, J. A. Strachan, and M. W. Kilimann. 1997. Autosomal glycogenosis of liver and muscle due to phosphorylase kinase deficiency is caused by mutations in the phosphorylase kinase beta subunit (PHKB). Hum. Mol. Genet. 6:1109–1115.

Buzała, M., M. Adamski, and B. Janicki. 2014. Characteristics of performance traits and the quality of meat and fat in Polish oat geese. Worlds Poult. Sci. J. 70:531–542.

Chen, S., J. An, L. Lian, L. Qu, J. Zheng, G. Xu, and N. Yang. 2013. Polymorphisms in AKT3, FIGF, PRKAG3, and TGF-β genes are associated with myofiber characteristics in chickens. Poult. Sci 92:325–330.

Chennaoui, M., P. Arnal, R. Dorey, F. Sauvet, S. Ciret, T. Gallopin, D. Leger, C. Drogou, and D. J. I. J. O. M. S. Gomez-merino. 2017. Changes of cerebral and/or peripheral adenosine A_1 receptor and IGF-I concentrations under extended sleep duration in rats. Int. J. Mol. Sci 18:2439.

Choe, J. H., Y. M. Choi, S. H. Lee, H. G. Shin, Y. C. Ryu, K. C. Hong, and B. C. Kim. 2008. The relation between glycogen, lactate content and muscle fiber type composition, and their influence on postmortem glycolytic rate and pork quality. Meat Sci 80:355–362.

Clark, A. S., W. E. Mitch, M. N. Goodman, J. M. Fagan, M. A. Goheer, and R. T. Curnow. 1987. Dichloroacetate inhibits glycolysis and augments insulin-stimulated glycogen synthesis in rat muscle. J. Clin. Invest 79:588–594.

Dewey, C. N., and B. J. B. B. Li. 2011. RSEM: accurate transcript quantification from RNA-Seq data with or without a reference genome. BMC Bioinf 12:323.

Fan, K., J. Wang, W. Sun, S. Shen, X. Ni, Z. Gong, B. Zheng, Z. Gao, X. Ni, T. Suo, H. Liu, and H. Liu. 2020. MUC16 C-terminal binding with ALDOC disrupts the ability of ALDOC to sense glucose and promotes gallbladder carcinoma growth. Exp. Cell. Res 394:112118.

Fidan, E. D., A. Nazlıgül, M. K. Türkyılmaz, S.Ü. Aypak, F. S. Kilimci, S. Karaarslan, and M. Kaya. 2017. Effect of photoperiod length and light intensity on some welfare criteria, carcass, and meat quality characteristics in broilers. Rev. Bras. Zootec 46:202–210.

Ganz, E., and H. K. Pauli. 1995. Whiteness and tint formulas of the Commission Internationale de l'Eclairage: approximations in the Lab color space. Appl. Opt. 34:2998–2999.

Gao, G., D. Gao, X. Zhao, S. Xu, K. Zhang, R. Wu, C. Yin, J. Li, Y. Xie, S. Hu, and Q. J. F. I. G. Wa. 2021a. Genome-wide association study-based identification of SNPs and haplotypes associated with goose reproductive performance and egg quality. Front. Genet 12:602583.

Gao, X., D. Zhao, L. Wang, Y. Cui, S. Wang, M. Lv, F. Zang, and R. Dai. 2021b. Proteomic changes in sarcoplasmic and myofibrillar proteins associated with color stability of ovine muscle during post-mortem storage. Foods 10:2989.

Ghosh, M., N. Sharma, A. K. Singh, M. Gera, K. K. Pulicherla, and D. K. Jeong. 2018. Transformation of animal genomics by next-generation sequencing technologies: a decade of challenges and their impact on genetic architecture. Crit. Rev. Biotechnol 38:1157–1175.

Haraf, G., J. Wołoszyn, A. Okruszek, Z. Goluch, M. Wereńska, and M. Teleszko. 2021. The protein and fat quality of thigh muscles from Polish goose varieties. Poult Sci 100:100992.

Heath, E., D. Tahri, E. Andermarcher, P. Schofield, S. Fleming, and C. A. Boulter. 2008. Abnormal skeletal and cardiac development, cardiomyopathy, muscle atrophy and cataracts in mice with a targeted disruption of the Nov (Ccn3) gene. BMC Dev. Biol 8:18.

House, G. M., E. B. Sobotik, J. R. Nelson, and G. S. Archer. 2021. Pekin duck productivity, physiological stress, immune response and behavior under 20L:4D and 16L:8D photoperiods. Appl. Anim. Behav. Sci 240:105351.

Hu, Z., J. Cao, G. Liu, H. Zhang, and X. Liu. 2020. Comparative transcriptome profiling of skeletal muscle from black muscovy duck at different growth stages using RNA-seq. Genes (Basel) 11:1228.

Jiang, W. Q., A. C. Chang, M. Satoh, Y. Furuichi, P. P. Tam, and R. R. Reddel. 2000. The distribution of stanniocalcin 1 protein in fetal mouse tissues suggests a role in bone and muscle development. J. Endocrinol 165:457–466.

Johnston, I., S. Manthri, A. Smart, P. Campbell, D. Nickell, and R. J. T. J. O. E. B. Alderson. 2003. Plasticity of muscle fibre number in seawater stages of Atlantic salmon in response to photoperiod manipulation. J. Exp. Biol 206:3425–3435.

Journal, J. K. J. W. S. P. S. 2021. Goose production and goose products. Worlds Poult. Sci. J 77:1–12.

Jung, Y. H., and S. Y. Bu. 2020. Suppression of long chain acyl-CoA synthetase blocks intracellular fatty acid flux and glucose uptake in skeletal myotubes. Biochim. Biophys. Acta Mol. Cell Biol. Lipids 1865:158678.

Kim, Y. S., J. S. Lee, Y. Lee, W. S. Kim, D. Q. Peng, M. H. Bae, Y. H. Jo, M. Baik, and H. G. Lee. 2018. Effect of glutamine on heat-shock protein beta 1 (HSPB1) expression during myogenic differentiation in bovine embryonic fibroblast cells. Food Sci. Biotechnol 27:829–835.

Kloet, F., J. Buurmans, M. J. Jonker, A. K. Smilde, and J. A. J. P. C. B. Westerhuis. 2020. Increased comparability between RNA-Seq and microarray data by utilization of gene sets. PLoS Comput. Biol 16:e1008295.

Kong, X., X. Wang, M. Li, W. Song, K. Huang, F. Zhang, Q. Zhang, J. Qi, and Y. He. 2021. Establishment of myoblast cell line and identification of key genes regulating myoblast differentiation in a marine teleost, Sebastes schlegelii. Gene 802:145869.

Lamosová, D., M. Zeman, and M. Juráni. 1998. Influence of melatonin on chick skeletal muscle cell growth. Comp. Biochem. Physiol. C Pharmacol. Toxicol. Endocrinol 118:375–379.

Lee, S., J. Shin, Y. Hong, M. Lee, K. Kim, S. R. Lee, K. T. Chang, and Y. Hong. 2012. Beneficial effects of melatonin on stroke-induced muscle atrophy in focal cerebral ischemic rats. Lab. Anim. Res 28:47–54.

Liu, G. J., Z. F. Chen, X. H. Zhao, M. Y. Li, and Z. H. Guo. 2020. Meta-analysis: supplementary artificial light and goose reproduction. Anim. Reprod. Sci 214:106278.

Lonergan, S. M., N. Deeb, C. A. Fedler, and S. J. Lamont. 2003. Breast meat quality and composition in unique chicken populations. Poult. Sci 82:1990–1994.

Love, M. I., W. Huber, and S. Anders. 2014. Moderated estimation of fold change and dispersion for RNA-seq data with DESeq2. Genome Biol 15:550.

Lew, C. R., S. Guin, and D. Theodorescu. 2015. Targeting glycogen metabolism in bladder cancer. Nat. Rev. Urol 12:383–391.

Mariné-casadó, R., C. Domenech-coca, J. Delbas, C. Bladé, L. Arola, and A. J. F. I. P. Caimari. 2018. The exposure to different photoperiods strongly modulates the glucose and lipid metabolisms of normoweight fischer 344 rats. Front. Physiol 9:416.

Men, X. M., B. Deng, X. Tao, Q. I. Ke-ke, and X. U. J. J. O. I. A. Zi-wei. 2017. Wnt gene expression in adult porcine longissimus dorsi and its association with muscle fiber type, energy metabolism, and meat quality. J. Integr. Agric. 16:144–150.

Mohan, A., M. C. Hunt, T. J. Barstow, T. A. Houser, and S. Muthukrishnan. 2010. Effects of malate, lactate, and pyruvate on myoglobin redox stability in homogenates of three bovine muscles. Meat Sci 86:304–310.

Mule, S. N., V. M. Gomes, R. A. M. Wailemann, J. Macedo-da-Silva, L. Rosa-fernandes, M. R. Larsen, L. Labriola, and G. Palmisano. 2021. HSPB1 influences mitochondrial respiration in ER-stressed beta cells. Biochim. Biophys. Acta Proteins Proteom 1869:140680.

Orkusz, A. 2021. Edible insects versus meat-nutritional comparison: knowledge of their composition is the key to good health. Nutrients 13:1207.

Orkusz, A., G. Haraf, A. Okruszek, and M. Werenska-sudnik. 2017. Lipid oxidation and color changes of goose meat stored under vacuum and modified atmosphere conditions. Poult. Sci. 96:731–737.

Perrin-cocon, L., P. O. Vidalain, C. Jacquemin, A. Aublin-gex, K. Olmstead, B. Panthu, G. J. P. Rautureau, P. Andre, P. Nyczka, M. T. Hutt, N. Amoedo, R. Rossignol, F. V. Filipp, V. Lotteau, and O. Diaz. 2021. A hexokinase isoenzyme switch in human liver cancer cells promotes lipogenesis and enhances innate immunity. Commun. Biol 4:217.

Puch-hau, C., I. Sánchez-tapia, V. Patiño-Suárez, M. Olvera-novoa, M. Gullian klanian, M. Quintanilla-mena, and O. J. M. Zapata-pérez. 2019. Isostichopus badionotusEvaluation of two independent protocols for the extraction of DNA and RNA from different tissues of sea cucumber. MethodsX 6:1627–1634.

Ren, J. M., B. A. Marshall, E. A. Gulve, J. Gao, D. W. Johnson, J. O. Holloszy, and M. Mueckler. 1993. Evidence from transgenic mice that glucose transport is rate-limiting for glycogen deposition and glycolysis in skeletal muscle. J. Biol. Chem. 268:16113–16115.

Robinson, M. D., D. J. Mccarthy, and G. K. J. B. Smyth. 2010. edgeR: a Bioconductor package for differential expression analysis of digital gene expression data. Bioinformatics 26:139–140.

Ropka-molik, K., A. Bereta, K. Żukowski, K. Piórkowska, A. Gurgul, and G. Żak. 2017. Transcriptomic gene profiling of porcine muscle tissue depending on histological properties. Anim. Sci. J 88:1178–1188.

Ropka-molik, K., A. Bereta, K. Żukowski, M. Tyra, K. Piórkowska, G. Żak, and M. Oczkowicz. 2018. Screening for candidate genes related with histological microstructure, meat quality and carcass characteristic in pig based on RNA-seq data. Asian-Australas. J. Anim. Sci 31:1565–1574.

Ryder, J. W., Y. Kawano, D. Galuska, R. Fahlman, H. Wallberg-henriksson, M. J. Charron, and J. R. Zierath. 1999. Postexercise glucose uptake and glycogen synthesis in skeletal muscle from GLUT4-deficient mice. FASEB J 13:2246–2256.

Starčević, M., H. Mahmutović, N. Glamočlija, M. Bašić, R. Andjelković, R. Mitrović, R. Marković, J. Janjić, M. Bošković, and M. J. A. A. I. J. O. A. B. Baltić. 2021. Growth performance, carcass characteristics, and selected meat quality traits of two strains of Pekin duck reared in intensive vs semi-intensive housing systems. Animal 15:100087.

Sun, J., X. Tan, X. Yang, L. Bai, F. Kong, G. Zhao, J. Wen, and R. Liu. 2022. Identification of candidate genes for meat color of chicken by combing selection signature analyses and differentially expressed genes. Genes (Basel) 13:307.

Tang, J., C. Faustman, T. A. Hoagland, R. A. Mancini, M. Seyfert, and M. C. Hunt. 2005. Postmortem oxygen consumption by mitochondria and its effects on myoglobin form and stability. J. Agric. Food Chem 53:1223–1230.

Torres-velarde, J. M., S. R. R. Kolora, J. I. Khudyakov, D. E. Crocker, P. H. Sudmant, and J. P. Vázquez-medina. 2021. Elephant seal muscle cells adapt to sustained glucocorticoid exposure by shifting their metabolic phenotype. Am. J. Physiol. Regul. Integr. Comp. Physiol 321:R413–R428.

Tuell, J. R., J. Y. Park, W. Wang, B. Cooper, T. Sobreira, H. W. Cheng, and Y. H. B. Kim. 2020a. Effects of photoperiod regime on meat quality, oxidative stability, and metabolites of postmortem broiler fillet (M. Pectoralis major) muscles. Foods 9:215.

Tuell, J. R., J. Y. Park, W. Wang, H. W. Cheng, and Y. H. B. Kim. 2020b. Functional/physicochemical properties and oxidative stability of ground meat from broilers reared under different photoperiods. Poult. Sci 99:3761–3768.

Wang, C., F. Yue, and S. Kuang. 2017. Muscle histology characterization using H&E staining and muscle fiber type classification using immunofluorescence staining. Bio. Protoc 7:e2279.

Wang, C. F., C. Z. Yuan, S. H. Wang, H. Zhang, X. X. Hu, L. Zhang, C. Wu, and N. Li. 2007. Differential gene expression of aldolase C (ALDOC) and hypoxic adaptation in chickens. Anim. Genet 38:203–210.

Wang, C. M., L. R. Chen, S. R. Lee, Y. S. Jea, and J. Y. Kao. 2009. Supplementary artificial light to increase egg production of geese under natural lighting conditions. Anim. Reprod. Sci 113:317–321.

Wang, H., M. Hu, Z. Ding, X. Zhou, S. Yang, Z. Shen, F. Yan, and A. Zhao. 2022. Phosphoglycerate dehydrogenase positively regulates the proliferation of chicken muscle cells. Poult. Sci 101:101805.

Wang, L., Z. Feng, X. Wang, X. Wang, and X. Zhang. 2010. DEGseq: an R package for identifying differentially expressed genes from RNA-seq data. Bioinformatics 26:136–138.

Watts, B. M., J. Kendrick, M. W. Zipser, B. Hutchins, and B. J. J. O. F. S. Saleh. 2010. Enzymatic reducing pathways in meat. J. Food Sci 31:855–862.

Wu, S. T., B. Liu, Z. Z. Ai, Z. C. Hong, P. T. You, H. Z. Wu, and Y. F. Yang. 2020. Esculetin inhibits cancer cell glycolysis by binding tumor PGK2, GPD2, and GPI. Front. Pharmacol 11:379.

Wüllrich-schmoll, A., and M. W. Kilimann. 1996. Structure of the human gene encoding the phosphorylase kinase beta subunit (PHKB). Eur. J. Biochem 238:374–380.

Xin, J., Z. Li, X. Li, M. Li, G. Li, W. Rao, and D. Zhang. 2018. Meat color stability of ovine muscles is related to glycolytic dehydrogenase activities. J. Food Sci 83:2432–2438.

Xu, T., Z. Xu, L. Lu, T. Zeng, L. Gu, Y. Huang, S. Zhang, P. Yang, Y. Wen, D. Lin, M. Xing, L. Huang, G. Liu, Z. Chao, and W. Sun. 2021. Transcriptome-wide study revealed m6A regulation of embryonic muscle development in Dingan goose (Anser cygnoides orientalis). BMC Genomics 22:270.

Yin, H., C. Cui, S. Han, Y. Chen, J. Zhao, H. He, D. Li, and Q. Zhu. 2020. Fibromodulin modulates chicken skeletal muscle development via the transforming growth factor-beta signaling pathway. Animals (Basel) 10:1477.

You, M., J. Liu, J. Zhang, M. Xv, and D. J. I. A. He. 2020. A novel chicken meat quality evaluation method based on color card localization and color correction. IEEE Access PP:2989439.

Zawilska, J. B., M. Berezińska, J. Rosiak, B. Vivien-roels, D. J. Skene, P. Pévet, and J. Z. Nowak. 2003. Daily variation in the concentration of melatonin and 5-methoxytryptophol in the goose pineal gland, retina, and plasma. Gen. Comp. Endocrinol 134:296–302.

Zhang, Y., J. Guo, Y. Gao, S. Niu, C. Yang, C. Bai, X. Yu, and Z. Zhao. 2014. Genome-wide methylation changes are associated with muscle fiber density and drip loss in male three-yellow chickens. Mol. Biol. Rep 41:3509–3516.

Zhao, Y., L. Zhang, M. Guo, and H. Yang. 2021. Taraxasterol suppresses cell proliferation and boosts cell apoptosis via inhibiting GPD2-mediated glycolysis in gastric cancer. Cytotechnology 73:815–825.